FVTD Thin-Wire Models Terminated by Arbitrary Lumped-Element Circuits

Ian Jeffrey and Joe LoVetri

Department of Electrical and Computer Engineering
University of Manitoba, Winnipeg, Manitoba, Canada R3T 5V6
ijeffrey@ee.umanitoba.ca, Joe_LoVetri@UManitoba.CA

Abstract: A thin-wire model which allows arbitrary lumped-element circuit terminations is described for the finite-volume time-domain (FVTD) discretization of Maxwell's equations. The model is based on the Holland-Simpson quasi-static formulation as extended by Edelvik for both the finite-difference and finite-element methods. This approach allows thin-wire 1D elements to be arbitrarily located within and independently of the FVTD volumetric mesh. A cell-centred flux-limited procedure, consistent with the FVTD update of the field variables, is used to discretize the thin-wire variables on the wire: charge/voltage and current. The voltage and charge variables are related via an assumed electrostatic field around the thin-wire. Thus, a unique voltage on the wire can be defined which allows one to introduce lumped-element terminations and junctions for thin-wire networks. The lumped-element circuits are formulated using modified nodal analysis where the interface to the thin-wires is handled as a set of auxiliary equations in the nodal description. It is shown how the thin-wire variables can be used to determine the reflection coefficient on a coaxial transmission line driving an electromagnetic structure.

Keywords: Thin-wire modeling, Finite-volume time-domain, Modified Nodal Analysis.

1. Introduction

The finite-volume time-domain (FVTD) technique considered herein is an electromagnetic field solver that discretizes Maxwell's equations using a cell-centered characteristic-based approach applicable on arbitrary unstructured meshes [1-3]. The current implementation of the University of Manitoba FVTD solver is capable of high-order numerical solutions on first-order meshes consisting of mixed element types such as tetrahedrons, hexahedrons and prisms. The solver has also been parallelized for distributed parallel computing environments by means of a modified orthogonal-recursive bisection (ORB) domain partitioning algorithm in conjunction with a halo/ghost element duplication scheme [4]. The parallel algorithm has shown excellent scalability, making it possible to solve very large computational problems. But even with state-of-the-art computational resources, the accurate volumetric modeling of such fine structures as thin wires and electronic circuitry is prohibitively expensive. Thus, it is important that sub-grid models be available for thin wires and that lumped-elements descriptions of the electronic circuitry be properly interfaced to the electromagnetic field solver.

We report on the development of a sub-grid thin-wire model for FVTD which includes lumped-element circuits at the terminal points of the wires. The thin-wire sub-grid model is an adaptation of Edelvik *et. al.*'s thin-wire model for the finite-difference time-domain (FDTD) and finite-element time-domain (FETD) algorithms [5, 6]. Edelvik's technique itself is based on the Holland-Simpson procedure for incorporating thin wires into an FDTD grid [7]. The method used for incorporating lumped element circuits at the termination points of the thin wires, which allows for the creation of junction points involving an arbitrary number of thin wires, uses the modified nodal-analysis (MNA) formulation [8]. Details of the FVTD

algorithm are available in [1-3], but sufficient detail is provided here so as to facilitate a description of the thin-wire model. In Section 2 and 3, we present the details of the thin-wire model for FVTD. Followed, in Section 4, by the MNA formulation of the lumped-element circuits that terminate the thin-wire. Here we point out that the voltage reference point is implied in the two models. In Section 5 we use these models to formulate the problem of a coaxial cable feeding a thin-wire dielectric resonator antenna (DRA) and show how the reflection coefficient S_{11} can be calculated using the thin-wire variables and provide useful results.

2. The FVTD Thin-Wire Model

Consider an infinitely-long straight wire of constant radius a oriented in the ζ-direction carrying a ζ-directed current $I = I(\zeta, t)$ and linear charge density ρ_l. Using cylindrical coordinates (r, ϕ, ζ), and assuming quasi-static fields produced by the current $I(\zeta, t)$, the spatial distributions of the fields are approximated as $E_r(r, \phi, \zeta, t) = \rho_l(\zeta, t)/(2\pi r\varepsilon)$ and $H_\phi(r, \phi, \zeta, t) = I(\zeta, t)/(2\pi r)$ where ε is the permittivity of the surrounding material. Substituting these quasi-static spatial distributions into Faraday's law and integrating radially from a to r for a fixed ζ, we obtain

$$(\mu_0/(2\pi))\ln(r/a)[c^2\partial_\zeta\rho_l(\zeta, t) + \partial_t I(\zeta, t)] = E_\zeta(r, \zeta, t), \tag{1}$$

where $v^{-2} = \varepsilon\mu_0$ is the speed of light in free-space, and ∂_ξ denotes partial differentiation with respect to ξ. Here we've used $E_\zeta(a, \zeta, t) = 0$ because the wire is assume to be a perfect electric conductor (PEC). To facilitate coupling the thin-wire variables to the external field it is desirable to remove this explicit r dependence and to replace it with a weighted average value throughout a circular disk concentric with the wire. Multiplying both sides of (1) by a weighting function $g(r)$, which has units m^{-2} and is zero for $r > r_0$, and integrating over the disk from $r = a$, the surface of the wire, to a model radius of $r = r_0$ gives

$$\mu_0\int_a^{r_0} rg(r)\ln(r/a)[c^2\partial_\zeta\rho_l(\zeta, t) + \partial_t I(\zeta, t)]dr = \langle E_\zeta(r, \zeta, t)\rangle, \tag{2}$$

where $\langle E_\zeta(r, \zeta, t)\rangle$ represents the weighted average of $E_\zeta(r, \zeta, t)$. The per-unit-length (PUL) inductance

$$L \triangleq \mu_0\int_a^{r_0} rg(r)\ln(r/a)dr \cong \frac{\mu_0}{2\pi}\ln\frac{r_0 + a}{2a}, \tag{3}$$

having dimensions $\mathrm{H/m}$, is defined for the wire. Note that this inductance depends on the weighting function $g(r)$ and r_0. A voltage is now defined in terms of the charge $\rho_l(\zeta, t)$ as $V(\zeta, t) \triangleq \rho_l(\zeta, t)/C$ using a PUL capacitance parameter $C \triangleq \varepsilon\mu_0/L = v^{-2}/L$. These definitions allow us to re-write (2) as

$$\partial_\zeta V(\zeta, t) + L\partial_t I(\zeta, t) = \langle E_\zeta(r, \zeta, t)\rangle. \tag{4}$$

Using conservation of charge along the wire, $\partial_\zeta I(\zeta, t) + \partial_t\rho_l(\zeta, t) = 0$, gives the second PDE:

$$\partial_\zeta I(\zeta, t) + C\partial_t V(\zeta, t) = 0. \tag{5}$$

Equations (4) and (5) are analogous to transmission-line equations for a transmission line having PUL parameters L and C and longitudinal source term $\langle E_\zeta(r, \zeta, t)\rangle$. It is important to note that this analogy arises only via the somewhat arbitrary definitions of PUL inductance and capacitance along the wire which allow us to define a voltage on the wire. A characteristic impedance for the "transmission-line" can also be defined as $Z_t = Y_t^{-1} = \sqrt{L/C}$.

3. Numerical Solution of the Thin-Wire Equations by FVTD

An arbitrary number of thin wires can be placed within the FVTD volumetric mesh each having its own uniform PUL quantities and oriented along its own direction ζ. The thin-wire transmission line equations are discretized using a 1D flux-split upwind FVTD scheme with MUSCL based flux-limiters [9]. The set of coupled PDEs, (4) and (5), for the voltage and current along a wire is written as a conservation law

$$\partial_t \boldsymbol{u}(\zeta, t) + \boldsymbol{A}\partial_\zeta \boldsymbol{u}(\zeta, t) = \boldsymbol{s}(\zeta, t), \tag{6}$$

where $\boldsymbol{u}(\zeta, t) = [V(\zeta, t), I(\zeta, t)]^T$, $\boldsymbol{s} = [0, L^{-1}\langle E_\zeta(r, \zeta, t)\rangle]^T$ is the source term, and

$$\boldsymbol{A} = \begin{bmatrix} 0 & C^{-1} \\ L^{-1} & 0 \end{bmatrix}. \tag{7}$$

Each wire is discretized into M wire segments (1D finite-volumes) of non-uniform length h_i and a solution $\boldsymbol{u}_i(\zeta, t)$ is associated with the centroid ζ_i of each wire segment $i = 1, \ldots, M$. Averaging (6) over each volume and applying the 1D divergence theorem gives

$$\partial_t \boldsymbol{u}_i(t) + h_i^{-1}\boldsymbol{A}(\boldsymbol{u}_{i+1/2}(t) - \boldsymbol{u}_{i-1/2}(t)) = \boldsymbol{s}_i(t), \tag{8}$$

where $\boldsymbol{u}_{i\pm 1/2}(t) \triangleq \boldsymbol{u}(\zeta_i \pm h_i/2, t)$ denotes the value of the solution vector at the "facet" between 1D cells. To evaluate the fluxes $\boldsymbol{f}_{i+1/2}(t) = \boldsymbol{A}\boldsymbol{u}_{i+1/2}(t)$ in (8) we use a flux-split, flux-limited upwind scheme for the spatial updating. The matrix $\boldsymbol{A}$ is diagonalizable as $\boldsymbol{A} = \Phi\Lambda\Phi^{-1} = \Phi(\Lambda^+ + \Lambda^-)\Phi^{-1} = \boldsymbol{A}^+ + \boldsymbol{A}^-$, where the matrices $\boldsymbol{A}^+ = \Phi\Lambda^+\Phi^{-1}$ and $\boldsymbol{A}^- = \Phi\Lambda^-\Phi^{-1}$ are constructed using the positive and negative eigenvalues, respectively. The orthogonal transformation matrices are easily determined as

$$\Phi = \begin{bmatrix} 1 & 1 \\ -Y_t & Y_t \end{bmatrix}, \quad \Phi^{-1} = \frac{1}{2}\begin{bmatrix} 1 & -Z_t \\ 1 & Z_t \end{bmatrix}, \tag{9}$$

and the diagonal eigenvalue matrix $\Lambda = \mathrm{diag}(c, -c)$ contains the speed of propagation along the line. Using this flux-splitting (8) can be written as

$$\partial_t \boldsymbol{u}_i(t) + h_i^{-1}[\boldsymbol{A}^+\boldsymbol{u}_{i+1/2}(t) - \boldsymbol{A}^+\boldsymbol{u}_{i-1/2}(t) + \boldsymbol{A}^-\boldsymbol{u}_{i+1/2}(t) - \boldsymbol{A}^-\boldsymbol{u}_{i-1/2}(t)] = \boldsymbol{s}_i(t). \tag{10}$$

Methods of approximating the solution at the facet depend on which operator, $\boldsymbol{A}^+$ or $\boldsymbol{A}^-$, will operate on that approximation. The simplest upwind approximation will take

$$\boldsymbol{A}^+\boldsymbol{u}_{i+1/2}(t) \approx \boldsymbol{A}^+\boldsymbol{u}_i(t),\ \boldsymbol{A}^+\boldsymbol{u}_{i-1/2}(t) \approx \boldsymbol{A}^+\boldsymbol{u}_{i-1}(t),\ \boldsymbol{A}^-\boldsymbol{u}_{i+1/2}(t) \approx \boldsymbol{A}^-\boldsymbol{u}_{i+1}(t),\ \boldsymbol{A}^-\boldsymbol{u}_{i-1/2}(t) \approx \boldsymbol{A}^-\boldsymbol{u}_i(t), \tag{11}$$

whereas higher order MUSCL-based flux limiters will interpolate the solution from the appropriate side [9].

4. Modified Nodal Analysis Formulation of Lumped Element Circuit Wire Terminations

For wires terminated by an electronic circuit we use an MNA formulation of the lumped-element description of the circuit. These circuits may be multiport networks that interconnect with multiple thin-wires or other types of transmission lines. This is best illustrated by example. Consider a circuit consisting of a single conductance G loading the far-end of a thin-wire. An MNA analysis of this simple circuit makes use of a single nodal voltage V_1, corresponding to the terminal voltage of the wire. Thus, there is an implied reference node N_{gnd} between the two models. The resulting equation is $GV_1 + I_{\mathrm{in},w} = 0$, where the current $I_{\mathrm{in},w}$ denotes the current leaving the node and travelling into wire. This is a single equation for the two unknowns: the nodal voltage at the line terminal, V_1, and the current into the wire, $I_{\mathrm{in},w}$. This wire current is not known because the solution values V, I on the wire segment are only known at the centroids of the 1D elements. Using a procedure similar to the one employed in [10], the characteristics variables on the line can be written in terms of the centroid voltage and current variables via the transformation

$$\omega_w = \begin{bmatrix} \omega_w^- \\ \omega_w^+ \end{bmatrix} = \Phi_w^{-1}\boldsymbol{u}_w = \begin{bmatrix} 1 & -Z_w \\ 1 & Z_w \end{bmatrix}\begin{bmatrix} V_w \\ I_w \end{bmatrix} = \begin{bmatrix} V_w - Z_w I_w \\ V_w + Z_w I_w \end{bmatrix}. \tag{12}$$

Thus, assuming we're dealing with the far-end of the wire, we can write the characteristic variable that is incoming to the terminal node from the wire as the positive-going characteristic variable. We can then approximate the characteristic variable at the far-end terminal, advanced by a half time-step, as

$$(\omega^{+}_{t,w})^{n+\Delta t/2} = (\omega^{+}_{N,w})^{n} = V^{n}_{N,w} + Z_w I^{n}_{N,w} = V^{n+\Delta t/2}_{t,w} + Z_w I^{n+\Delta t/2}_{t,w} = V^{n+\Delta t/2}_{1} - Z_w I^{n+\Delta t/2}_{\text{in},w}, \quad (13)$$

where subscript N refers to the centroid of the last element on the wire w, and subscript t refers to the terminal of wire w. This allows us to write the MNA update equations as

$$\begin{bmatrix} -Z_w & 1 \\ 1 & G \end{bmatrix} \begin{bmatrix} I_{\text{in},w} \\ V_1 \end{bmatrix}^{n+\Delta t/2} = \begin{bmatrix} \omega^{+}_{N,w} \\ 0 \end{bmatrix}^{n}, \quad (14)$$

which can be solved for the unknown quantities $V^{n+\Delta t/2}_{1}$ and $I^{n+\Delta t/2}_{\text{in},w}$. These quantities can then be used to compute the incoming flux into the cell at the $(n+1)^{\text{th}}$ time step.

The process is similar with more complicated circuits. Consider a Thévenin voltage source located at the near-end of a wire as shown in Fig. 1 (where now the incoming characteristic variable will be the negative travelling characteristic variable). The MNA update equation becomes

$$\begin{bmatrix} -Z_w & 0 & 1 & 0 \\ 0 & 0 & 0 & 1 \\ 1 & 0 & G & -G \\ 0 & 1 & -G & G \end{bmatrix} \begin{bmatrix} I_{\text{in},w} \\ I_T \\ V_1 \\ V_2 \end{bmatrix}^{n+\Delta t/2} = \begin{bmatrix} \omega^{-}_{1,w} \\ V_T \\ 0 \\ 0 \end{bmatrix}^{n}. \quad (15)$$

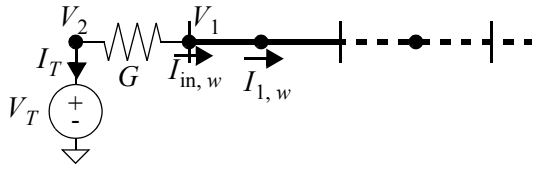

Fig. 1. Near-end Thévenin source driving thin-wire.

In general, an MNA description compatible with the 1D cell-centered update scheme consists of: *one auxiliary unknown input current for each thin-wire element connected to the circuit*, *one auxiliary unknown branch current for each voltage source present in the circuit*, *one nodal voltage for each input and/or internal node in the circuit excluding the reference node*. Corresponding to each of these unknowns the MNA description provides the following equations: *one equation for each node connected to a thin-wire relating the input current and nodal voltage at the input node to the incoming flux at the wire element centroid; one equation that relates each imposed voltage source to the nodal voltages it connects to; one equation for enforcing conservation of current (charge) at each input/internal node excluding the ground node where the presence of voltage sources connected to the nodes is incorporated via the auxiliary branch current for that voltage source.*

5. Numerical Results for Modeling a Coaxial Transmission Line

An important use of the thin-wire model is the simulation of a coaxial cable that feeds an arbitrary electromagnetic structure. As such, we first demonstrate the simulation of a terminated coaxial cable and then show results for a coaxial cable feeding a dielectric-resonator antenna (DRA).

If we want to model a matched termination using a lumped element circuit model, the question arises as to what the termination impedance should be. To answer this question, we note that although the voltage

on the thin-wire model is not the same as the effective voltage on the coaxial cable, the PUL charge on the thin-wire is the same as the effective charge on the modelled inner-conductor of the cable. Thus, $Q = C_c V_c = C_t V_t$, where the subscripts "c" and "t" refer to variables on the modelled coaxial cable and thin-wire, respectively. The current I will be the same in the two models and, because the velocity of propagation for the thin-wire model is the same as for cable, the characteristic impedances are similarly related as $v_0^{-1} = C_c Z_c = C_t Z_t$. Using these relationships, we note that the reflection coefficient, S_{11}, can be calculated using either the thin-wire variables or the cable variables:

$$S_{11} = \frac{V_c - Z_c I}{V_c + Z_c I} = \frac{(C_c/C_t)(V_t - Z_t I)}{(C_c/C_t)(V_t + Z_t I)} = \frac{V_t - Z_t I}{V_t + Z_t I}. \tag{16}$$

To obtain an equivalent S_{11} on a cable due to an actual load impedance Z_L, the equivalent termination on the thin-wire model needs to be set as $Z_{Leq} = (C_c/C_t)Z_L = (Z_t/Z_c)Z_L$. Thus, to match the cable, one needs to terminate the thin-wire model in its characteristic impedance. This analysis was verified using numerical experiments for an air-filled 40 mm long coaxial cable with inner-conductor radius $a = 0.63$ mm and outer conductor radius $b = 2.25$ mm. The characteristic impedance of the coaxial cable is $Z_0 = 76.3\ \Omega$. The inner-conductor was modelled as a thin-wire extending the length of the cable using 79 1D elements and the interior of the cable was modelled using 4179 tetrahedral elements. The model interaction radius was chosen as $r_0 = 2.22$ mm, almost to the outer conductor. This gives a characteristic impedance for the equivalent thin-wire transmission line, calculated via (3), of $Z_t = 49.3\ \Omega$. A lumped-element source having a Thévenin source inpedance also matched to the line was used to excite the line. Numerical results for the matched line produced an $S_{11} < -10$dB up to 6 GHz.

The next example is a DRA similar to the one described in [11], having the dimensions shown in Fig. 2 and fed by the same coaxial transmission line described previously (except that now the thin-wire modelling the inner conductor starts a 5 mm distance inside the outer conductor). The mesh consisted of 21,954 vertices, 1 0D element (for the source point), 81 1D elements (for the thin-wire), 5320 2D elements (for the PEC surfaces), and 125,175 3D tetrahedral elements. The lumped-element voltage source feeding the line was the derivative of a Gaussian pulse having appreciable energy well above 6 GHz. The calculated S_{11} for various observation points on the coaxial cable below the ground plane are shown in Fig. 2. The distance below the ground plane is listed in the legend of the figure. Notice that the reflection coefficient changes depending on the location of the observation point. This is due to the higher-order modes that may exist close to the feed point of the antenna (*i.e.*, at the ground plane).

6. Conclusions

A thin-wire model for use in FVTD field solvers which allows lumped-element circuits to be modelled at the terminations of the wire, or the junctions between wires, has been described. The model has been evaluated by comparing results for an ideally matched coaxial cable and the S_{11} of a DRA. It has been shown how the voltage and current variables along the wire can be used to determine the reflection coefficient.

References

[1] D. Firsov, J. LoVetri, I. Jeffrey, V. Okhmatovski, C. Gilmore, W. Chamma "High-Order FVTD on Unstructured Grids using an Object-Oriented Computational Engine," *ACES J.*, vol. 22, no. 1, pp. 71-82, 2007.

[2] D. Firsov, I. Jeffrey, J. LoVetri, C. Gilmore "An Object Oriented Finite-Volume Time-Domain Computational Engine," *2006 ACES Conference*, Miami, Florida, pp. 211-218, March 2006.

[3] P. Bonnet, X. Ferrieres, P.L. Michielsen, P. Klotz "Finite Volume Time Domain Method," in *Time Domain Electromagnetics,* S.M. Rao, Academic Press, San Diego, 1999.

[4] I. Jeffrey, D. Firsov, C. Gilmore, V. Okhmatovski, J. LoVetri "Parallel High-Order EM-FVTD on an Unstructured Mesh*," 2007 ACES Conference*, Verona, Italy, pp. 401-408, March 2007.

[5] F. Edelvik, G. Ledfelt, P. Lötstedt, D.J. Riley "An unconditionally stable subcell model for arbitrarily oriented thin wires in the FETD method," *IEEE Trans. AP*, vol. 51, no. 8, pp. 1797-1805, Aug. 2003.

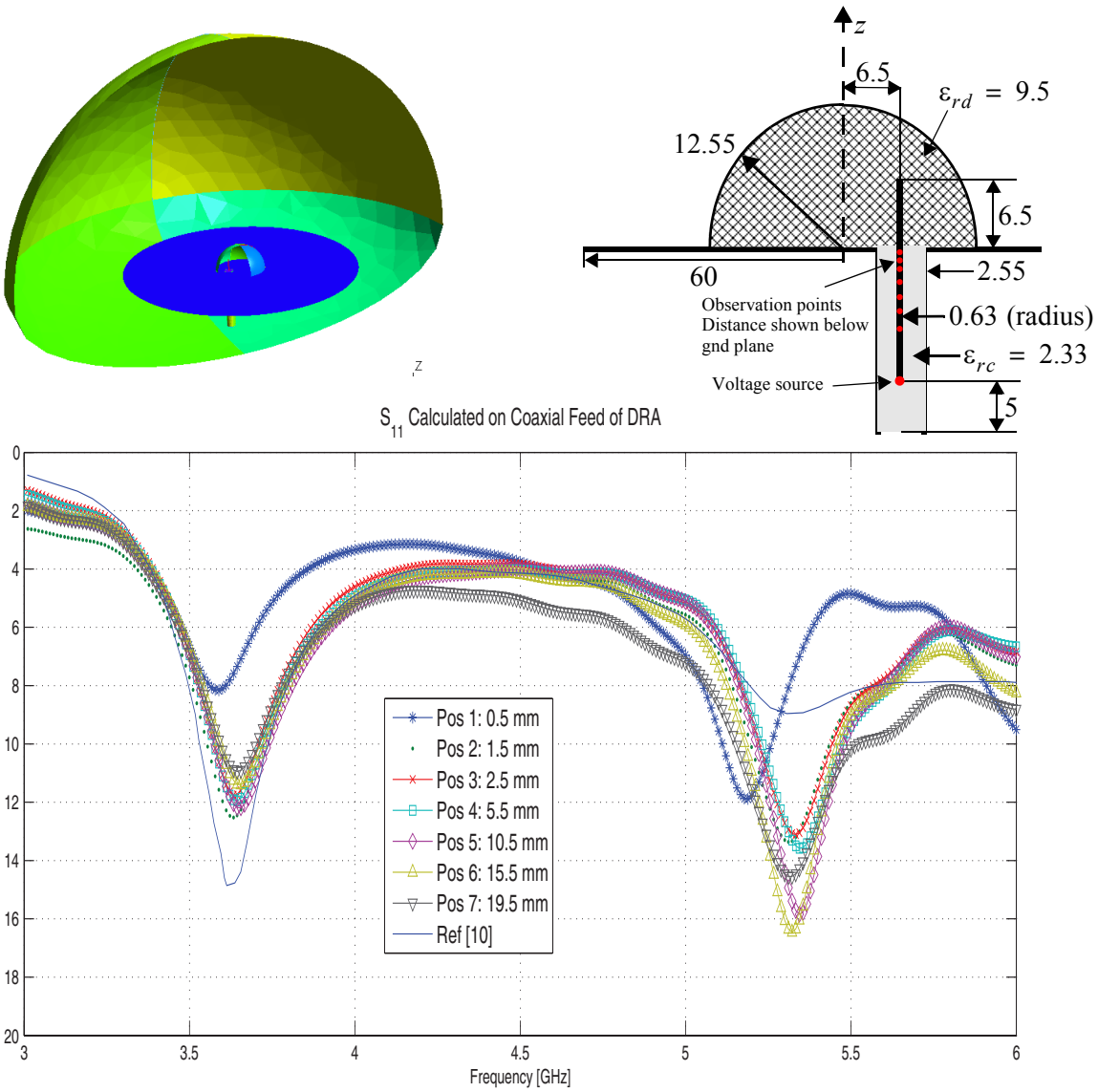

Fig. 2. DRA fed by a coaxial cable (units in mm). Top-left: mesh, Top-right: geometry, Bottom: plot of S11 using voltage on the thin-wire observed at different locations below the ground plane.

[6] F. Edelvik "A new technique for accurate and stable modeling of arbitrarily oriented thin wires in the FDTD method," *IEEE Trans. EMC*, vol. 45, no. 2, pp. 416-423, May 2003.

[7] R. Holland, L. Simpson "Finite-difference analysis of EMP coupling to thin struts and wires", *IEEE Trans. EMC*, vol. 23, no. 2, pp. 88-97, May 1981.

[8] J. Vlach, K. Singhal, *Computer Methods for Circuit Analysis and Design*, 2nd Ed., Van Nostrand, 1994.

[9] B. van Leer, "Towards the ultimate conservative difference schemes, V, A second order sequel to Godunov's method," *J. of Comp. Physics*, vol. 32, pp. 101-136, 1979.

[10] J. LoVetri and T. Lapohos, "Explicit upwind schemes for lossy MTLs with linear terminations," *IEEE Trans. on EMC*, vol. 39, no. 3, pp. 189-200, Aug. 1997.

[11] C. Fumeaux, D. Baumann, R. Vahldieck, "Advanced FVTD Simulation of Dielectric Resonator Antennas and Feed Structures," *ACES J.*, vol. 19, no. 3, pp. 155-164, Nov. 2004.